

Theoretical studies of energy–energy correlation in e^+e^- annihilation

N.K. Falck* and G. Kramer

II. Institut für Theoretische Physik der Universität Hamburg, D-2000 Hamburg 50, Federal Republic of Germany

Received 10 August 1988

Abstract. We calculate the $O(\alpha_s^2)$ correction to the energy–energy correlation cross section in e^+e^- annihilation using different resolution criteria in the limit of vanishing resolution cuts. We compare this in the back-to-back angular region with results of the logarithm approximation (LA) and deduce higher order corrections (beyond $O(\alpha_s^2)$) from the LA formula. The final results are compared with recent TASSO data.

1 Introduction

The measurement of energy–energy correlation (EEC) in e^+e^- annihilation has been used quite frequently as a possible test of perturbative QCD. Experimentally, one measures the energy weighted correlation defined by

$$\frac{1}{\sigma} \frac{d\Sigma}{d \cos \chi} = \frac{2}{W^2 \Delta \chi \sin \chi} \frac{1}{N} \sum_{A=1}^N \sum_{\substack{\text{pairs in} \\ \Delta \chi}} E_{Aa} E_{Ab} \quad (1.1)$$

where χ is the relative angle between two calorimeters and the index A specifies the event (1 to N), while a and b specify the individual particles. To compare with perturbative QCD one then calculates the same quantity for quarks and gluons. The collinear configurations are removed by looking at angles χ , between quarks and gluons, such that $\chi \neq 0^\circ, 180^\circ$. Due to the energy weighting the rapid variation of the QCD matrix elements is tempered in the region of small parton momenta.

In QCD perturbation theory the correlation function Σ is written up to second order in α_s as

$$\frac{1}{\sigma_0} \frac{d\Sigma}{d \cos \chi} = \frac{\alpha_s}{\pi} C(\cos \chi) + \left(\frac{\alpha_s}{\pi}\right)^2 D(\cos \chi) \quad (1.2)$$

where σ_0 is the total annihilation cross section in

zeroth order of α_s . The first order term receives its contribution from the well-known one-gluon emission diagrams [1]. The second order term $D(\cos \chi)$ receives contributions from graphs with $q\bar{q}g$ and $q\bar{q}q\bar{q}$ final states and also from graphs which consist of virtual corrections to the $q\bar{q}g$ final state. These $O(\alpha_s^2)$ 3- and 4-parton cross sections are individually infrared and collinear divergent. To cancel these singularities several methods have been invented which give similar results. One finds that $D/C \simeq 5-10$ over the whole range of $\cos \chi$, so that, since $(\alpha_s/\pi) \simeq 0.05$, the $O(\alpha_s^2)$ correction is appreciable and leads to an increase of up to 50% compared to the lowest order result [2–4]. The $O(\alpha_s^2)$ cross section (1.2) is useful only for χ values away from $\chi = 0^\circ, 180^\circ$. In the limiting back-to-back ($\chi \rightarrow 180^\circ$) and collinear ($\chi \rightarrow 0^\circ$) regions the two functions $C(\cos \chi)$ and $D(\cos \chi)$ diverge. To study the behaviour of the EEC in these limiting regions one must go beyond perturbation theory of finite order and try to sum up all terms up to finite order. This can be done by summing the most singular contributions to the EEC in the respective limits. Of course, this leading logarithm summation is valid only in the nearest vicinity of $\chi = 0^\circ$ and $\chi = 180^\circ$ and cannot be applied for large angles away from the forward or backward direction, respectively. In order to obtain a reasonable approximation of the EEC over all angles one can try to combine the logarithmic approximation (LA) with the finite order results. To be more specific, let us consider the combination of the LA in the limit $\chi \rightarrow 180^\circ$ with finite order results in the following form

$$\frac{1}{\sigma_0} \frac{d\Sigma}{d \cos \chi} = \frac{1}{\sigma_0} \frac{d\Sigma}{d \cos \chi} \Big|_{LA} + X(\cos \chi) \quad (1.3)$$

where $X(\cos \chi)$ contains all terms of (1.2) not already contained in $(1/\sigma_0)(d\Sigma/d \cos \chi)$ after expansion in powers of α_s up to α_s^2 . Then (1.3) has the correct behaviour for $\chi \rightarrow 180^\circ$ (this will be given later) and agrees with (1.2), if expanded in powers of α_s up to $O(\alpha_s^2)$. One might hope that (1.3) will be a better representation of the EEC in QCD than (1.2), since

* Supported by Bundesministerium für Forschung und Technologie, 05 4HH 92P (3), Bonn, FRG

near $\chi = 180^\circ$ it is corrected by an infinite power series in α_s , although only valid for angles very near to the back-to-back direction. In this region the logarithms are large and one might hope that their sum represents a good approximation to the EEC for angles near the backward direction. Away from the backward direction (1.3) agrees with (1.2) up to $O(\alpha_s^2)$ terms and the higher order terms contained in the LA term in (1.3) constitute some correction. The many large logarithmic factors in the LA term come from the infrared, soft gluon region. There has been considerable theoretical effort for controlling these logarithmic factors and sum them to all order in α_s [5]. In this work we shall employ the representation of the LA term and supplement them with the higher order results represented by (1.2). This way we obtain a representation of the EEC which is valid not only for small back-to-back angles (i.e. of order $180^\circ - \chi$) but also for large angles up to angles near the collinear region due to the term $X(\cos \chi)$ in (1.3).

If one discusses the limiting behaviour for $\cos \chi \rightarrow -1$ it is useful to define a variable $\eta = \frac{1}{2}(1 + \cos \chi)$ and to include in the LA term all singular terms in the limit $\eta \rightarrow 0$, i.e. all terms proportional to $1/\eta$. Then X has the property that it contains all contributions such that

$$\lim_{\eta \rightarrow 0} \eta X(\cos \chi = 2\eta - 1) = 0. \quad (1.4)$$

This procedure was followed easily by many authors when combining the summed LA, which is the first term in (1.3), with the lowest order term, i.e. the term $(\alpha_s/\pi)C(\cos \chi)$ in (1.2) (see (2.1) for $C(\cos \chi)$) since the singular terms of C are known explicitly (see (2.2)). Unfortunately the singular terms of $D(\cos \chi)$, i.e. the terms proportional to η^{-1} , are not firmly established. The reason being that $D(\cos \chi)$ has been obtained only numerically. Although some contributions of $D(\cos \chi)$ have been calculated analytically, of which we shall present examples in the next section, the complete result of D is produced only through extensive numerical integrations using Monte-Carlo routines. The largest effort to establish the singular behaviour of D for $\eta \rightarrow 0$ has been made by Ellis et al. [3]. They found that the two most singular terms proportional to $\ln^3(1/\eta)/\eta$ and to $\ln^2(1/\eta)/\eta$ agree with the corresponding $O(\alpha_s^2)$ terms of the LA but that the $\ln(1/\eta)/\eta$ term already differs from the predicted LA term (the term $1/\eta$ is not predicted in the LA approach). Since even the agreement of the leading and the next sub-leading term could be verified only inside very large errors we consider the problem whether $D(\cos \chi)$ as calculated numerically in [3] agrees in the most singular terms ($\sim 1/\eta$) with the LA as unsolved. Since the numerical evaluation of D is particular problematic for small η there is little hope that the singular behaviour of D for $\eta \rightarrow 0$ will be known in the future. In addition the evaluation of $D(\cos \chi)$ is not unique, since there are several methods, how to cancel infrared and collinear divergences between virtual and real

$O(\alpha_s^2)$ corrections. This might have bearing in particular on the third leading term of $D(\cos \chi)$ for $\eta \rightarrow 0$ proportional to $\ln(1/\eta)/\eta$. Therefore we propose a more pragmatic procedure. We start with (1.3) and calculate the LA term as it appears in the literature [5] and determine $X(\cos \chi)$ in (1.3) from our evaluation of (1.2) minus the terms up to $O(\alpha_s^2)$ contained already in the LA-term of (1.3). In this form we have a representation of the EEC with reasonable behaviour for $\eta \rightarrow 0$ which agrees with the higher order evaluation up to terms proportional to α_s^2 . In this form we give up the property (1.4). Our $X(\cos \chi)$ might still contain sub-leading singular terms in the $O(\alpha_s^2)$ contribution. Only part of them is contained in the LA-term. In this framework the LA term has been considered only in connection with the $O(\alpha_s)$ contribution to $X(\cos \chi)$. Then there is no problem to obey (1.4) since the $O(\alpha_s)$ term is known analytically and its singular part coincides with the $O(\alpha_s)$ part of the LA-term. It is the purpose of this work to extend (1.3) in such a way that it includes the complete $O(\alpha_s^2)$ term in the whole η range. This way we can learn something about higher order corrections ($\alpha_s^n (n \geq 3)$) in the small η range and can study how (1.3) behaves in the limit $\eta \rightarrow 0$. The range of small η is also heavily influenced by hadronization effects of quarks and gluons. Since the effects diminish with increasing beam energy it is particularly important to know the modification of the ECC in the small η range through higher order terms.

The outline of our work is as follows. In sect. 2 we discuss different approaches for calculating the higher order term $D(\cos \chi)$ in (1.2) and compare the results to them. Section 3 contains the formulas for the LA contribution in (1.3) and the numerical results for the EEC based on (1.3) with one particular form for D from Sect. 2. These results are compared with recent results from the TASSO collaboration at PETRA.

2 $O(\alpha_s^2)$ Corrections to the EEC

In this section we describe different methods for calculating $D(\cos \chi)$ as defined in (1.2) and compare their results. First we present results based on resolution dependent cross sections for 3 and 4 jets. This is an extension of earlier work of Schneider et al. [4]. Then we consider results from [2] and [3] where the EEC was calculated directly without defining jet cross sections.

The first order term $C(\cos \chi)$ in (1.2) receives its contribution from the well known one gluon emission diagrams and reads [1]

$$C(\cos \chi) = \frac{C_F}{8} \frac{3 - 2\zeta}{\zeta^5(1 - \zeta)} \cdot [2(3 - 6\zeta + 2\zeta^2)\ln(1 - \zeta) + 3\zeta(2 - 3\zeta)] \quad (2.1)$$

where $\zeta = \frac{1}{2}(1 - \cos \chi) = 1 - \eta$. Its singular approximation in the limit $\eta \rightarrow 0$ is

$$C(\cos \chi)_{LA} = \frac{C_F}{4\eta} (\ln(1/\eta) - \frac{3}{2}). \quad (2.2)$$

The second order term $D(\cos \chi)$ in (1.2) receives its contributions from graphs with $q\bar{q}gg$ and $q\bar{q}q\bar{q}$ final states and from all graphs which consist of the virtual corrections to the $q\bar{q}g$ final state. These 4- and 3-parton cross sections are individually infrared and collinear divergent. To cancel these singularities several methods are available. One possibility is to define cross sections for the production of 3- and 4-jets and then calculate the EEC for jets. Such jet cross sections are resolution dependent. For example, the 3-jet cross section to order α_s^2 is

$$d\sigma^{3\text{-jet}}(\varepsilon, \delta) = d\sigma^{3\text{-parton}} + d\sigma^{4\text{-parton}}(\varepsilon, \delta) \quad (2.3)$$

where $d\sigma^{3\text{-parton}}$ is the $O(\alpha_s^2)$ contribution with $q\bar{q}g$ in the final state, and where $d\sigma^{4\text{-parton}}$ stands for the cross section for $e^+e^- \rightarrow q\bar{q}gg$ and $e^+e^- \rightarrow q\bar{q}q\bar{q}$, in which two of the 4 partons are not resolved. As resolution we can take, for example, the Sterman–Weinberg criteria. Then two partons are not resolved, if the two partons lie inside a cone of (full) opening angle δ and/or the energy of one of the two partons is $\leq \varepsilon W/2$. This resolution dependent 3-jet cross section has been calculated analytically in an approximation where subleading terms which are not needed for the cancellation of infrared and collinear singularities had been neglected [6]. It depends on the two scaled energies for quark and antiquark $x_i = 2E_i/W$ ($i = 1, 2$) like the lowest order 3-jet cross section. It is straightforward to calculate the EEC from it. Since subleading terms which give contributions proportional to ε and δ have been neglected, $d\sigma^{3\text{-jet}}(\varepsilon, \delta)$ is reliable only for *very small* ε, δ -values. To obtain the complete EEC the genuine (hard) 4-jet contributions $d\sigma^{4\text{-jet}}(\varepsilon, \delta)$ must be added. It is the cross section for the production of 4 partons which fails the ε, δ cuts, and which is obtained by simple Monte-Carlo integration. This part is exact and includes all $O(\varepsilon)$ and $O(\delta)$ terms. Altogether $D(\cos \chi)$ is given in this scheme by

$$D(\cos \chi) = \int dP_3 \sum_{i,j=1}^3 \frac{E_i E_j}{W^2} \delta(\hat{\mathbf{p}}_i \hat{\mathbf{p}}_j - \cos \chi) \frac{d\sigma^{3\text{-jet}}(\varepsilon, \delta)}{dP_3} \\ \cdot \int dP_4 \sum_{i,j=1}^4 \frac{E_i E_j}{W^2} \delta(\hat{\mathbf{p}}_i \hat{\mathbf{p}}_j - \cos \chi) \frac{d\sigma^{4\text{-jet}}(\varepsilon, \delta)}{dP_4} \quad (2.4)$$

where $dP_3(dP_4)$ denotes the 3-body (4-body) phase space integration for massless quanta. Both $d\sigma^{3\text{-jet}}(\varepsilon, \delta)$ and $d\sigma^{4\text{-jet}}(\varepsilon, \delta)$ depend on ε and δ ; the 3-jet cross section decreases for $\varepsilon, \delta \rightarrow 0$ like $(-\ln \varepsilon \ln \delta)$ whereas the 4-jet cross section increases like $\ln \varepsilon \ln \delta$. In the sum (2.4) this strong ε, δ dependence, together with the subdominant single logarithmic terms $\sim \ln \varepsilon$ and $\sim \ln \delta$, is expected to cancel, so that the sum (2.3) has a finite limit for $\varepsilon, \delta \rightarrow 0$. This was checked numerically for the inclusive thrust distribution in [7]. In [4] $C(\cos \chi)$ and $D(\cos \chi)$ have been calculated for two

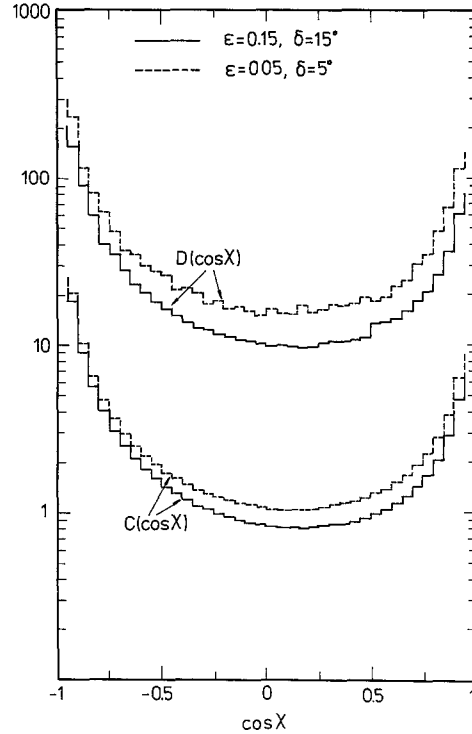


Fig. 1. First and second order contributions $C(\cos \chi)$ and $D(\cos \chi)$ to the energy–energy correlation for $\varepsilon, \delta = 0.05, 5^\circ$ and $\varepsilon, \delta = 0.15, 15^\circ$ as a function of $\cos \chi$

values of ε, δ , i.e. $\varepsilon, \delta = 0.15, 15^\circ$ and $\varepsilon, \delta = 0.05, 5^\circ$. It was found that $C(\cos \chi)$ increased somewhat with decreasing ε, δ . This change is due to the separation of the 2-jet contribution from the 3-jet ($q\bar{q}g$) final state. In $D(\cos \chi)$ the variation with ε, δ was found to be stronger. Part of this variation comes again from the change in the 2-jet contribution. The other part originates from the fact that in the calculation of $d\sigma^{3\text{-jet}}(\varepsilon, \delta)$ sub-leading terms proportional to ε and δ had been neglected [8]. In this paper we are interested to know the limit of (2.3) for $\varepsilon, \delta \rightarrow 0$. For this purpose and to compare with the earlier results we have calculated $C(\cos \chi)$ and $D(\cos \chi)$ for $\varepsilon, \delta = 0.15, 15^\circ; 0.05, 5^\circ$ and $0.01, 1.5^\circ$. We have plotted $C(\cos \chi)$ and $D(\cos \chi)$ for $\varepsilon, \delta = 0.15, 15^\circ$ and $\varepsilon, \delta = 0.05, 5^\circ$ in Fig. 1* and for $\varepsilon, \delta = 0.01, 1.5^\circ$ in Fig. 2. We see that $C(\cos \chi)$ in Fig. 1 changes by 30%, whereas $D(\cos \chi)$ increases by 60%, if we go from the higher to the lower ε, δ values. This shows that a large fraction of the change in D is due to the separation of different 2-jet contributions which is the only reason for the ε, δ -dependence of $C(\cos \chi)$. The result for $D(\cos \chi)$ at $\varepsilon, \delta = 0.01, 1.5^\circ$ is not very accurate due to appreciable Monte-Carlo fluctuations. But inside the fluctuations

* The results for $\varepsilon, \delta = 0.15, 15^\circ$ and $\varepsilon, \delta = 0.05, 5^\circ$ differ from the results in [4] for the same ε, δ . In [4] easy to calculate subleading terms proportional to $\varepsilon \ln \delta$ were kept. In [8] it was found that such terms are cancelled by other subleading contributions. Therefore we left them out here. We checked that these $\varepsilon \ln \delta$ terms of [4] were negligible for $\varepsilon, \delta = 0.01, 1.5^\circ$

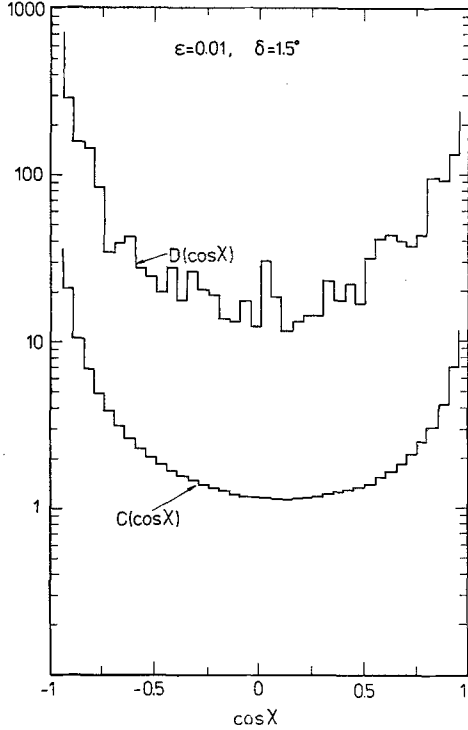


Fig. 2. Same as Fig. 1 for $\varepsilon, \delta = 0.01, 1.5^\circ$

it agrees approximately with the result for $\varepsilon = 0.05$, $\delta = 5^\circ$. This means, that for small enough ε, δ values $D(\cos \chi)$ is independent of ε, δ and we can consider the result in Fig. 2 as the limit for $\varepsilon, \delta \rightarrow 0$. For comparison of different methods we write (1.2) in the following form

$$\frac{1}{\sigma_0} \frac{d\Sigma}{d \cos \chi} = \frac{\alpha_s}{\pi} C(\cos \chi) \left(1 + \frac{\alpha_s}{\pi} R(\cos \chi) \right). \quad (2.5)$$

We have plotted $R(\cos \chi)$ for $\varepsilon = 0.05$, $\delta = 5^\circ$ in Fig. 3, the corresponding curve for $\varepsilon = 0.01$, $\delta = 1.5^\circ$ is similar, but with much larger Monte Carlo fluctuations.

A second possibility to cancel infrared and collinear singularities is to calculate (2.3), but with a different resolution approach to separate 3-jet from 4-jet production. An even simpler than the (ε, δ) resolution is the invariant mass resolution. In this case two partons i, j are irresolvable if $(p_i + p_j)^2/W^2 \leq y$. By 3-jet cross section we then understand the cross section for events which consist of three clusters, each having an invariant mass squared smaller than yW^2 . In analogy to the case with ε, δ -cuts $d\sigma^{4\text{-jet}}(y)$ is the cross section for $e^+ e^- \rightarrow q\bar{q}gg + q\bar{q}q\bar{q}$ with $(p_i + p_j)^2 \geq yW^2$ for all combinations $i, j = 1, 2, 3, 4$. Then $D(\cos \chi)$ is calculated from (2.4) with ε, δ cuts replaced by the y cut. Both cross sections $d\sigma^{3\text{-jet}}(y)$ and $d\sigma^{4\text{-jet}}(y)$ depend on y . $d\sigma^{3\text{-jet}}(y)$ decreases with decreasing y like $(-\ln^2 y)$, whereas the $d\sigma^{4\text{-jet}}(y)$ increases like $\ln^2 y$. In the sum (2.4) these and the y dependent subdominant terms $\sim \ln y$ should cancel. This was checked for the inclusive thrust distribution on [7]. To see how $D(\cos \chi)$ changes with the y resolution and to check whether it

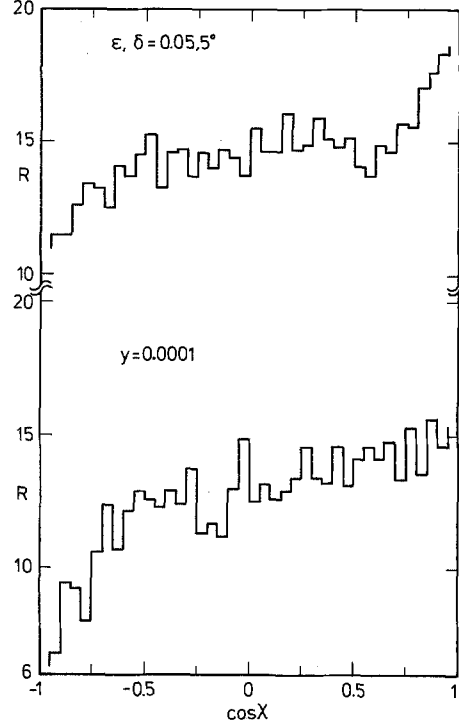


Fig. 3. Ratio $R(\cos \chi)$ of second to first order contribution as a function of $\cos \chi$ for $\varepsilon, \delta = 0.05, 5^\circ$ and $y = 0.0001$

approaches the same limit for small enough y values as $D(\cos \chi)$ obtained with ε, δ resolution above we have done the evaluation of $D(\cos \chi)$ for $y = 0.01, 0.001$ and 0.0001 . The formulas for $d\sigma^{3\text{-jet}}(y)$ are taken from [7]. They are not complete since subdominant terms $O(y)$ could not be calculated analytically and had been neglected. For the $d\sigma^{3\text{-jet}}(y)$ of [7], which depend on the scaled energies $x_i = 2E_i/W$ ($i = 1, 2$), we were able to do the integrals analytically and to obtain the 3-jet part of $D(\cos \chi)$ directly. The result is written down in Appendix A. These formulae are useful to investigate the asymptotic behaviour for $\chi \rightarrow 180^\circ$, which is also given in this appendix.

We present the results for $C(\cos \chi)$ and $D(\cos \chi)$ for $y = 0.01$ and 0.001 in Fig. 4 and for $y = 0.0001$ in Fig. 5. The lowest order result $C(\cos \chi)$ is somewhat different from the C in Fig. 1 since with the y cut the 2-jet contribution is defined differently as compared to the ε, δ -cut. We notice that $C(\cos \chi)$ changes very little if we go from $y = 0.01$ to $y = 0.001$ except in the small χ region where $C(\cos \chi)$ is reduced if y is increased. This sensitivity of $C(\cos \chi)$ for small angles on the y cut was also noticed in [2]. Also $D(\cos \chi)$ changes less with varying y (see Fig. 4) as compared to the $D(\cos \chi)$ with varying ε, δ in Fig. 1. But $D(\cos \chi)$ is also influenced more for small angles if y is increased. If we compare $D(\cos \chi)$ for $y = 0.001$ in Fig. 4 with $D(\cos \chi)$ for $y = 0.0001$ we see that $D(\cos \chi)$ increases by less than 10% with decreasing y . In Fig. 3 we have plotted R for $y = 0.0001$. This can be compared to R calculated for $\varepsilon = 0.05$, $\delta = 5^\circ$. We see that both R 's have approximately the same shape as a function of $\cos \chi$. R

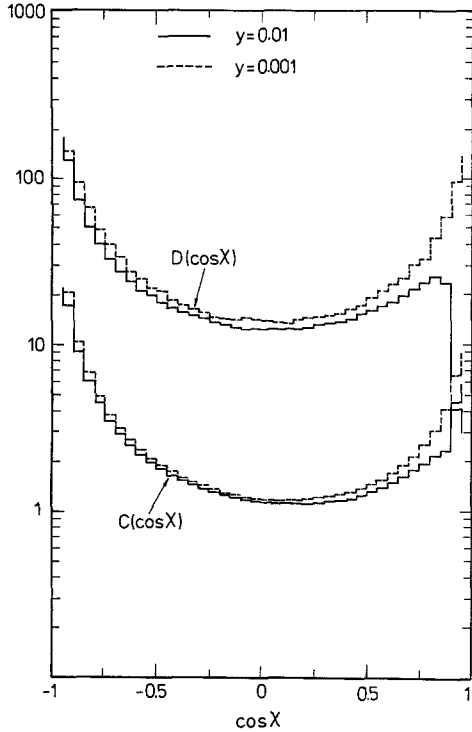


Fig. 4. Same as Fig. 1 for invariant mass cuts $y = 0.01$ and $y = 0.001$

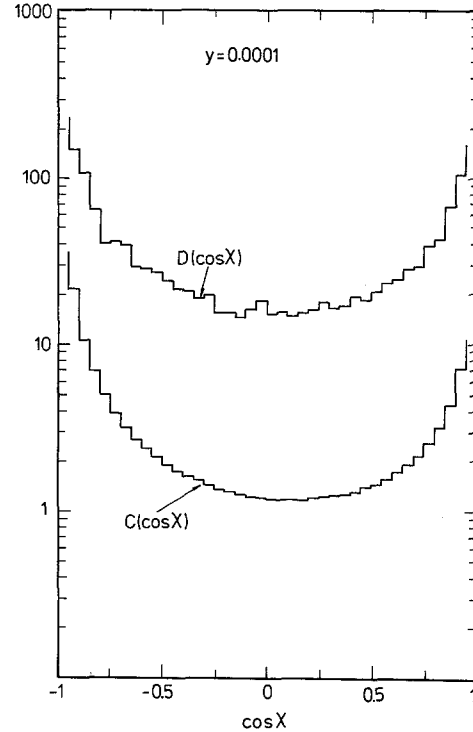


Fig. 5. Same as Fig. 1 for invariant mass cut $y = 0.0001$

increases if we change χ from 180° to $\chi = 0^\circ$. But R with the ε, δ cut is still approximately 15% larger (for example in the interval $\cos \chi \in [-0.25, 0.25]$) although $\varepsilon = 0.05$, $\delta = 5^\circ$ would correspond more to the y -cut value $y = 0.001$ ($\varepsilon^2 \simeq \delta^2/4 \simeq y$). On the other hand $C(\cos \chi)$ for $\varepsilon = 0.05$ and $\delta = 5^\circ$ is still 10% smaller than $C(\cos \chi)$ for $y = 0.0001$. If we had divided by the limiting $C(\cos \chi)$ the two R 's in Fig. 3 would agree reasonably well. It seems that with the method based on y cuts one can obtain more stable results for $D(\cos \chi)$ than with comparable ε, δ -cuts (compare Fig. 2 with Fig. 5) if the same amount of Monte-Carlo runs are done. In the following we shall take $D(\cos \chi)$ for $y = 0.0001$ as the limit of $D(\cos \chi)$ with resolution cut going to zero and combine it with the summed LA results in the next section. Instead of this $D(\cos \chi)$ we could have used the corresponding result of [2] or [3]. We prefer our result since it has been obtained with two essentially independent methods.

Now we compare our $D(\cos \chi)$ with $y = 0.0001$ to results of other authors using a different method for cancelling infrared and collinear singularities. So Ali and Barreiro [2] and Ellis et al. [3] base their evaluation of $D(\cos \chi)$ on the following formula [2]

$$d\sigma = d\sigma_{\text{virt}} + \int_0^{y_{\text{max}}} dy_{ij} \frac{d\phi}{2\pi} [d\sigma_4(y_{ij}^{-1} \text{ piece})]. \quad (2.6)$$

The integral in (2.6) is done by writing

$$d\sigma_4 = d\sigma_4^s + [d\sigma_4 - d\sigma_4^s]. \quad (2.7)$$

The singular piece $d\sigma_4^s$ is obtained by integrating

analytically the singular contribution of $d\sigma^{4\text{-parton}}$ in (2.6) with the appropriate upper limit of integration y_{max} and is combined with the contribution of the virtual corrections $d\sigma_{\text{virt}}$. The resulting formulae are derived in [9]. The result is $d\sigma_3$. It depends on the two 3-jet variables x_1 and x_2 . By integrating over one of these variables the contribution to the EEC can be derived also analytically. The result is given in Appendix B, where also the asymptotic behaviour for $\eta \rightarrow 0$ is evaluated. The integral for the square bracket in (2.7) can be calculated only numerically, usually with a lower limit y_0 on the integration of all invariants y_{ij} (in [2] $y_0 = 10^{-7}$ is used). We can rewrite (2.6) with the lower limit y_0 in the following form

$$d\sigma = d\sigma_{\text{virt}} + \int_0^{y_0} dy_{ij} \frac{d\phi}{2\pi} [d\sigma_4(y_{ij}^{-1} \text{ piece})] + \int_{y_0}^{y_{\text{max}}} dy_{ij} \frac{d\phi}{2\pi} [d\sigma_4(y_{ij}^{-1} \text{ piece})]. \quad (2.8)$$

By choosing $y_0 = 10^{-4}$ the third term in (2.8) is identical to the 4-jet part in (2.4) with ε, δ replaced by y_0 . The first and second term in (2.8) can be obtained from our 3-jet contribution for $y = 0.0001$ by leaving out one term which corresponds to a subleading contribution originating from symmetric integration to produce the correct 3-jet cross section (for a more complete discussion see [8]). Furthermore in the range $0 \leq y_{ij} \leq y_0$ the full $d\sigma^4$ is approximated by $d\sigma_4^s$. The result of such a calculation is shown in Fig. 6, where we plotted $R(\cos \chi)$. In this approach R has the same

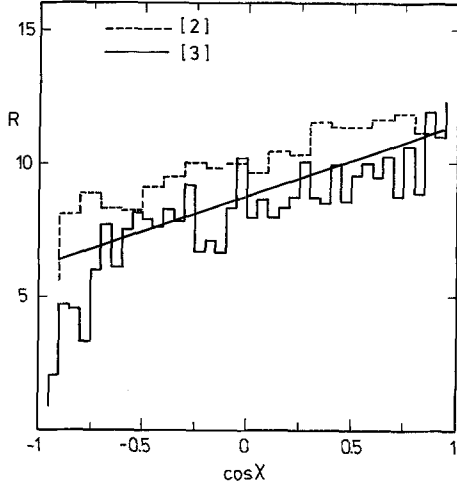


Fig. 6. Ratio $R(\cos\chi)$ of second to first order contribution as a function of $\cos\chi$ for direct approach without using jet cross sections compared to results of [2] and [3]

dependence on $\cos\chi$ as the R in Fig. 3 but it is approximately 50% smaller (at $\cos\chi = 0$ we have $R \simeq 8$ as compared to $R \simeq 12.5$ in Fig. 3). On the other hand R in Fig. 6 agrees rather well with the result from Ellis et al. [3] and somewhat less with the results of Ali et al. [2]. Ellis et al. [3] and Ali et al. [2] employed the same method for calculating R . So their results should coincide. They differ roughly by one unit in R . It is conceivable that the difference comes either from using different values for the lower limit y_0 or different Monte-Carlo routines. We conclude from this that the lower cut $y_0 = 10^{-4}$ seems to be sufficient and that for $y_{ij} \leq y_0$ the 4-parton cross section can be approximated by the singular contribution $d\sigma_4^s$. The difference of R in Fig. 3 as compared to Fig. 6 can only be attributed to the fact, that in the approach which we used to compute R in Fig. 3, we made use of a different definition for $d\sigma^{3\text{-jet}}$ than by using (2.7). We think that further work is necessary for establishing the ultimate higher order EEC. Since the results for R obtained in the different approaches still differ somewhat it seems premature to say something definite about the singular behaviour of R for $\eta \rightarrow 0$.

3 Leading logarithms in the EEC

In this section we present the summed leading logarithm formulae for the EEC and establish their α_s expansion up to $O(\alpha_s^2)$. By subtracting this $O(\alpha_s^2)$ expansion we obtain the LA correction for small η which is added to $D(\cos\chi)$ obtained in Sect. 2.

The summed to all orders of α_s leading logarithm approximation of the EEC is given by the Bessel transform (to incorporate the conservation of transverse momentum) [10]

$$\frac{1}{\sigma_0} \frac{d\Sigma}{d\cos\chi} \Big|_{LA} = \frac{1}{16} \int_0^\infty dz J_0(\sqrt{z\eta}) e^{v(z)} \quad (3.1)$$

where the exponent $v(z)$ has a perturbative expansion

of the following form

$$v(z) = \sum_{N=1}^{\infty} \sum_{M=0}^{N+1} D_{NM} \left(\frac{\alpha_s(W^2)}{\pi} \right)^N \left(\ln \frac{z}{z_0} \right)^M \quad (3.2)$$

z_0 stands for $e^{2(\ln 2 - \gamma)}$ where γ is Euler's constant (0.57721...). The coefficients D_{NM} have been calculated by several groups [5]. Best understood are the terms for $M = N + 1$. The first term D_{12} yields the usual double leading logarithm approximation (DLA). The higher terms with $M = N + 1$ are simply generated from D_{12} as a result of the running of the coupling constant. The subleading terms with $M = N$ are less understood. In total the coefficients known so far are [5, 11]:

$$\begin{aligned} D_{12} &= -\frac{1}{2} C_F, & D_{11} &= \frac{3}{2} C_F, & D_{10} &= -C_F \left(2 + \frac{\pi^2}{6} \right) \\ D_{23} &= \frac{b_0}{3} D_{12}, \\ D_{22} &= \frac{3}{8} C_F b_0 - \frac{C_F}{4} \left[N_c \left(\frac{67}{18} - \frac{\pi^2}{6} \right) - \frac{5}{3} N_f \right] \end{aligned} \quad (3.3)$$

where $b_0 = (11N_c - 2N_f)/6$, $N_c = 3$, $C_F = 4/3$. $\alpha_s(W^2)$ is supposed to be given by the well-known two-loop formula. The coefficients D_{21} and D_{20} are unknown as well as all higher D_{NM} with $N \geq 3$. The perturbative expansion of (3.1) with $v(z)$ is easily calculated from

$$\frac{1}{\sigma_0} \frac{d\Sigma}{d\cos\chi} \Big|_{LA} = -\frac{1}{8\eta} \int_0^\infty dz \sqrt{\eta z} J_1(\sqrt{\eta z}) v'(z) e^{v(z)} \quad (3.4)$$

using the techniques of [10]. The expansion is written as

$$\frac{1}{\sigma_0} \frac{d\Sigma}{d\cos\chi} \Big|_{LA} = \frac{1}{\eta} \sum_{N=1}^{\infty} \sum_{M=0}^{2N-1} C_{NM} \left(\frac{\alpha_s(W^2)}{\pi} \right)^N \left(\ln \frac{1}{\eta} \right)^M \quad (3.5)$$

Then the expansion coefficients are given in terms of the D_{NM} . Up to $N = 2$ they are [3]:

$$\begin{aligned} C_{11} &= -\frac{1}{2} D_{12} = \frac{1}{4} C_F, \\ C_{10} &= -\frac{1}{4} D_{11} = -\frac{3}{8} C_F, \\ C_{23} &= -\frac{1}{2} D_{12}^2 = -\frac{1}{8} C_F^2 \\ C_{22} &= -\frac{3}{4} D_{23} - \frac{3}{4} D_{12} D_{11} \\ &= \frac{1}{8} C_F \left(\frac{9}{2} C_F + \frac{11}{6} N_c - \frac{1}{3} N_f \right) \\ C_{21} &= -\frac{1}{2} D_{22} - \frac{1}{4} D_{11}^2 - \frac{1}{2} D_{12} D_{10} \\ &= \frac{1}{8} C_F \left[-\left(\frac{17}{2} + \frac{\pi^2}{3} \right) C_F \right. \\ &\quad \left. + \left(\frac{35}{36} - \frac{\pi^2}{6} \right) N_c - \frac{1}{18} N_f \right] \\ C_{20} &= -\frac{1}{4} D_{21} - \frac{1}{4} D_{11} D_{10} + \frac{\pi^2}{3} D_{12}^2 \\ &= -\frac{1}{4} D_{21} + \frac{1}{8} C_F^2 \left(6 + \frac{\pi^2}{2} + 4\zeta_3 \right). \end{aligned} \quad (3.6)$$

Since D_{21} is not known we put $D_{21} = 0$ in the following. As mentioned we see explicitly in (3.6) that all coefficients except C_{21} are expressible through D_{12}, D_{11}, D_{10} and b_0 . This means they are generated from the lowest order term through exponentiation and through the running coupling constant α_s .

We can compare the LA expansion of the singular part of the EEC, this is the EEC deduced from (2.6) and $d\sigma_4$ replaced by $d\sigma_4^s$, with the coefficients in (3.6). In Appendix B we obtained for the $O(\alpha_s^2)$ coefficients, where ζ_3 is the usual ζ -function: $\zeta_3 = 1.202057$:

$$\begin{aligned} C_{23} &= \frac{1}{8} C_F \left(-\frac{2}{3} C_F - \frac{1}{6} N_c \right) \\ C_{22} &= \frac{1}{8} C_F \left(3C_F + \frac{11}{6} N_c - \frac{1}{3} N_f \right) \\ C_{21} &= \frac{1}{8} C_F \left[-\left(\frac{15}{4} + \frac{4}{3} \pi^2 \right) C_F + \left(\frac{53}{36} + \frac{\pi^2}{2} \right) N_c - \frac{1}{18} N_f \right] \\ C_{20} &= \frac{1}{8} C_F \left[-\left(\frac{233}{24} - \frac{35\pi^2}{9} \right) C_F \right. \\ &\quad \left. - \left(\frac{155}{24} + \frac{7\pi^2}{9} + 2\zeta_3 \right) N_c + \left(\frac{11}{12} - \frac{\pi^2}{9} \right) N_f \right]. \end{aligned} \quad (3.7)$$

Now we can compare the C_{ij} in (3.7) with those in (3.6). Since D_{21} is unknown in the LA this can be done only for C_{23}, C_{22} and C_{21} . We see that only the N_c and the N_f term in C_{22} agrees. This is one of the terms proportional to b_0 which in the LA is generated through the running α_s . Another term of this sort appears in C_{21} originating from D_{22} in (3.3). This cannot be checked since other terms proportional to N_c and N_f are present. But the N_f -term agrees nevertheless. But the leading terms C_{23} (the C_F and N_c -part) and C_{22} (only C_F -part) do not agree. We have checked by direct numerical integration that the missing C_F and N_c -terms in C_{23} and C_{22} , namely $C_F^2/24$ and $C_F N_c/48$ in C_{23} and $\frac{3}{16} C_F^2$ in C_{22} are generated from (2.6) when we replace $d\sigma_4$ in (2.6) by the second term in (2.7), i.e. the non-singular 4-parton contribution $d\sigma_4 - d\sigma_4^s$. But we were unable to verify the missing terms in C_{21} from numerical integration of $d\sigma_4 - d\sigma_4^s$. But, of course, there is some uncertainty in this method. In [3] the C_{21} term was checked by a very detailed numerical integration of $d\sigma_4 - d\sigma_4^s$. These authors found, compared to (3.6), an additional term in C_{21} equal to $-\frac{1}{8} C_F (25 \pm 6)$ which reduces the value of C_{21} appreciably. On the other hand they also found a very positive term in C_{20} if compared to C_{20} in (3.6) with $D_{21} = 0$, so that these two additional terms cancel each other to a large extent except when η is extremely small. Due to the fact that Ali et al. [2] and Ellis et al. [3] differ in the result of $D(\cos \chi)$, although using the same method, we have doubts that it is possible to determine accurately subleading terms in (3.5) by numerical integrations, although the authors in [3] did a very thorough numerical analysis to substantiate their claim.

In the following we shall disregard the problem whether our $D(\cos \chi)$ has the same singular terms for $\eta \rightarrow 0$ as those in (3.5) and (3.6). We take the point of view that for very small η the EEC is given by (3.4) with $v(z)$ taken from (3.2) and (3.3). Then the perturbative expansion of this EEC might come close to the full perturbative EEC as obtained in Sect. 2 in all terms up to C_{22} .

Before we calculate the correction of the EEC for small η with the summed up LA in (3.4) we compare numerically the perturbative expansion of (3.4), i.e. (3.5) with coefficients (3.6) with the full perturbative EEC from Sect. 2. This is shown in Fig. 7 where we have plotted $C(\cos \chi)$ and $D(\cos \chi)$ as defined in (1.2) and obtained with $y = 10^{-4}$, as already shown in Fig. 5, which are compared to C and D calculated from (3.5) and (3.6). All functions are plotted only for $\cos \chi$ smaller than 0.5, since only for small η we can expect some similarity. Both C and D in LA seem to approach the complete C and D for $\cos \chi \rightarrow -1$. C in LA becomes negative for $\cos \chi > -0.6$, as is obvious from (2.2). Therefore C in LA can be used only for small η , i.e. $\cos \chi < -0.8$. This property of C is well-known and forbids the application of the LA and the summed LA for larger η values. D in LA stays positive but deviates also from the complete D for $\cos \chi > -0.8$. This qualitative behaviour of the LA in comparison with the complete perturbative (up to $O(\alpha_s^2)$) expansion does not change if we sum the LA using (3.4). To see this explicitly we must make a choice for $\alpha_s(W^2)$. We take $\alpha_s(W^2) = 0.14$, which is a reasonable coupling in the PETRA-PEP energy range. In Fig. 8 we exhibited $(1/\sigma_0)(d\Sigma/d\cos \chi)$ with the complete $O(\alpha_s) + O(\alpha_s^2)$ terms obtained in Sect. 2 and the corresponding curve in LA together with the summed LA. In Fig. 8 we observe that the summed LA and the perturbative LA are very similar. Both are sensible only for $\cos \chi < -0.5$. They differ appreciably from the complete EEC for $\cos \chi > -0.8$. Furthermore the LA to all orders is always larger than the perturbative LA, at least for $\cos \chi > -0.95$, so that, if we correct the complete perturbative EEC with LA to all orders minus perturbative LA, the correction is positive and not too large as can be read off from Fig. 8. The three curves in Fig. 8 are extended to smaller η (with smaller $\cos \chi$ intervals averaged) down to $\cos \chi = -0.99$ in Fig. 9. The perturbative LA approaches the complete perturbative EEC further. The difference between summed LA and perturbative LA changes sign at $\cos \chi \simeq -0.97$. But this difference is still small compared to the complete perturbative EEC. Therefore for moderate χ , i.e. $\cos \chi > -0.99$ the complete perturbative EEC is still a very accurate result. The significance of the summed LA lies in the fact that it is needed for extrapolation to $2\eta = (1 + \cos \chi) \rightarrow 0$. This can be seen in Fig. 10 where the perturbative LA is compared with the summed LA as a function of $1 + \cos \chi$ between 10^{-5} and 10^{-1} . Down to $(1 + \cos \chi) = 3 \cdot 10^{-4}$ the perturbative LA and the

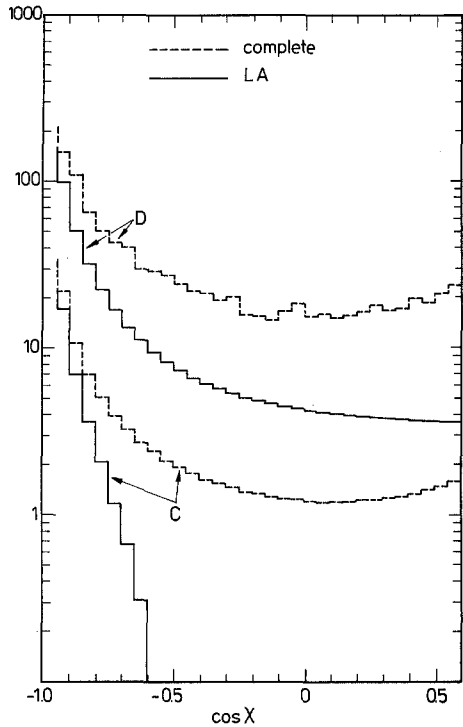


Fig. 7. Comparison of the first and second order LA (see (3.5) and (3.6)) with the complete C and D of Fig. 5

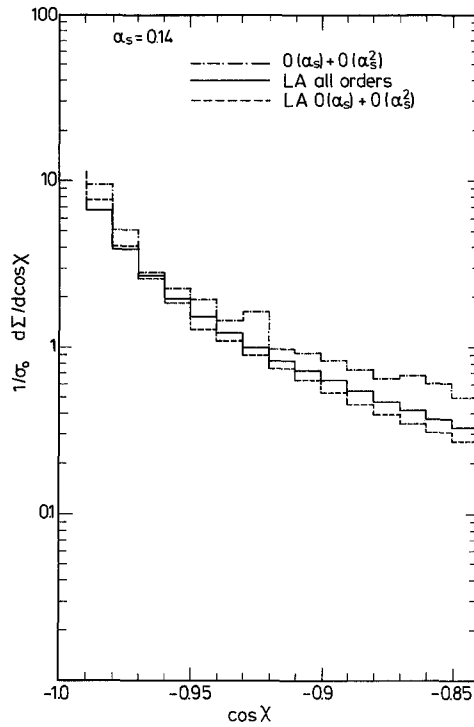


Fig. 9. Same as Fig. 8 for smaller $\cos \chi$ intervals and nearer to large angle limit

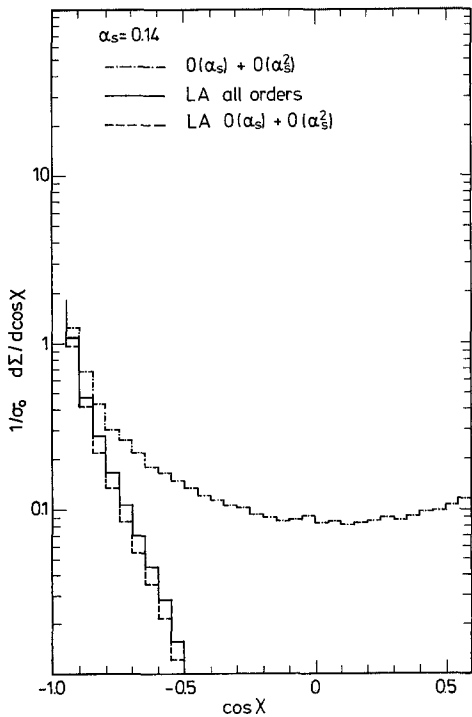


Fig. 8. Comparison of the energy-energy correlation in perturbative LA and LA to all orders with complete energy-energy correlation calculated from C and D in Fig. 5 for $\alpha_s = 0.14$ as a function of $\cos \chi$

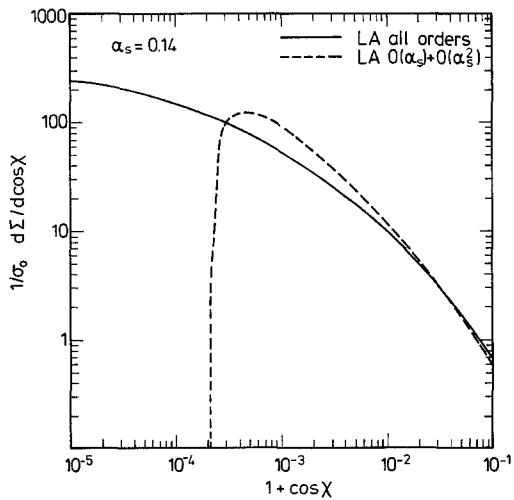


Fig. 10. Comparison of the energy-energy correlation for perturbative LA and for LA to all orders as a function of $(1 + \cos \chi)$ for angles very near to the back-to-back limit

summed LA (both for $\alpha_s = 0.14$) are very similar. For $(1 + \cos \chi) = 2 \cdot 10^{-4}$ the perturbative LA diverges to $-\infty$, whereas the summed LA converges to a finite limit for $\eta \rightarrow 0$. Between $2\eta = 10^{-2}$ and $2\eta = 10^{-5}$ the EEC in summed LA still increases by a factor 25. Since it seems impossible to calculate numerically the complete perturbative EEC for very small η values a reasonable approximation to the EEC for all angles might be: i) use the perturbative EEC for $\cos \chi$ above (-0.99) , say, and replace it for $\cos \chi \leq -0.99$ by the

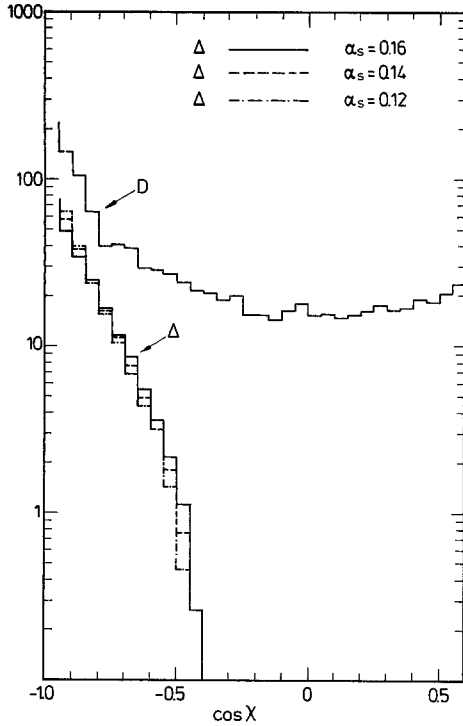


Fig. 11. Higher order (α_s^n , $n \geq 3$) correction term Δ originating from the summed logarithmic approximation as defined in the text and for $\alpha_s = 0.12, 0.14$ and 0.16 as a function of $\cos \chi$ compared to D of Fig. 5

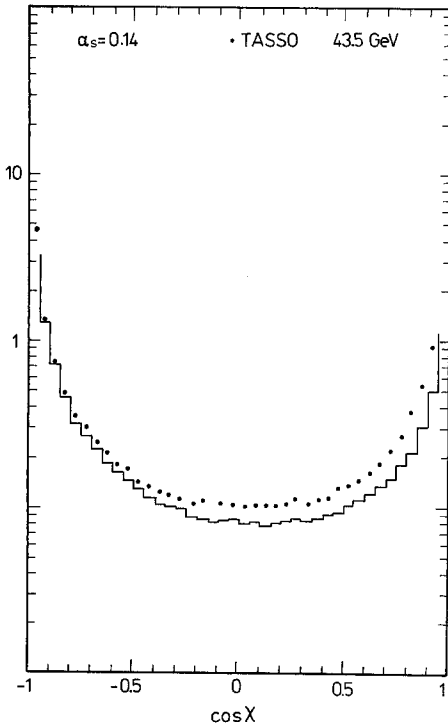


Fig. 12. Comparison of the energy–energy correlation for $\alpha_s = 0.14$ corrected with the Δ contribution of Fig. 11 compared to TASSO data [12]

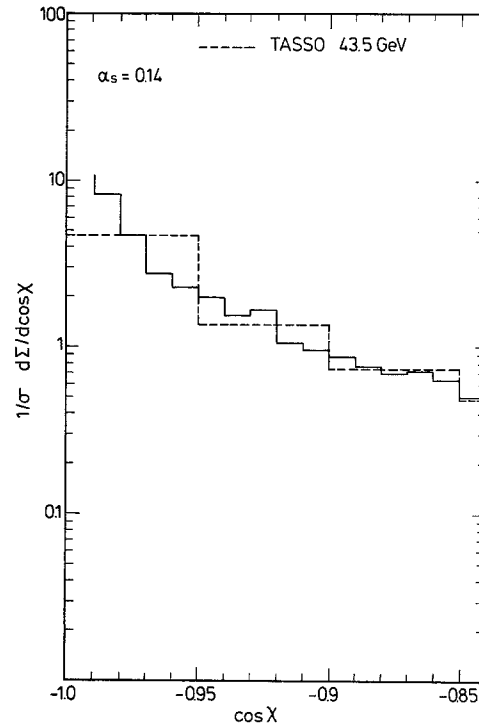


Fig. 13. Same as Fig. 12 for smaller $(1 + \cos \chi)$ and smaller $\cos \chi$ intervals

summed logarithmic approximation obtained from (3.4). of course, this procedure corrects just the limiting behaviour of the EEC for $\eta \rightarrow 0$ via the summed LA. Actually we want to improve the EEC also for finite although small η . For this purpose we have calculated Δ which is the EEC according to (3.4) minus the EEC based on (3.5) and (3.6), i.e. the perturbative LA, both multiplied with $(\alpha_s/\pi)^{-2}$

$$\Delta = \left(\frac{\pi}{\alpha_s}\right)^2 [\text{LA}(\text{all orders}) - \text{LA}(O(\alpha_s) + O(\alpha_s^2))]. \quad (3.8)$$

Then Δ is the higher order correction to $D(\cos \chi)$ for small η ($\eta \leq 0.25$). It is plotted in Fig. 11 for $\alpha_s = 0.12, 0.14$ and 0.16 (it depends on α_s since (3.4) has terms $O(\alpha_s^n)$ with $n \geq 3$). Depending on the $\cos \chi$ interval Δ constitutes a correction to D between 5% and 30%. For the smallest η 's the correction is largest. The curve for Δ as presented in Fig. 11 is our main result (Fig. 8 and Fig. 9 contain the same information for $\alpha_s = 0.14$). It shows that the higher order corrections $O(\alpha_s^n)$ with $n \geq 3$ are not very large of the order of 10% for $\cos \chi$ between -0.99 and -0.85 and smaller for larger $\cos \chi$.

The effect of Δ on the complete EEC for a realistic α_s can be seen by comparing the curves in Figs. 12 and 13 with the curves labelled $O(\alpha_s) + O(\alpha_s^2)$ in Figs. 8 and 9. We see that the difference is astonishingly small. This means that the fixed order calculation is much more reliable than anticipated. Of course, our

proposal, to replace at extremely small η the EEC by the summed LA term makes sense only, if the $O(\alpha_s^2)$ singular terms in $D(\cos \chi)$ agree with the LA. This might be the case but has not been proven jet. In case they deviate one could correct the LA by the extra terms. In case these extra terms are in subleading contributions, as, for example, found in [3], this will hardly change Δ in the very small η region ($\cos \chi < -0.99$). If on the other hand the $D(\cos \chi)$, as used here, differs from the LA in the $O(\alpha_s^2)$ asymptotic terms the ansatz (1.3) is useless for establishing the behaviour of the EEC for $\eta \rightarrow 0$, since X would still contain divergent terms for $\eta \rightarrow 0$. Since it is unlikely that all singular terms of D will ever be known the best strategy is to use $D(\cos \chi)$ up to such $\cos \chi$ where it equals the LA term and then extrapolate with the LA down to $\eta = 0$.

In Figs. 12 and 13 we compare our final prediction with recent experimental data of the TASSO Collaboration for $E_{c.m.} = 43.5 \text{ GeV}$ [12]*. In Fig. 13 the small η region is plotted separately. We see that the experimental data agree with the theoretical curve reasonably well, in particular in the small η region. Actually we can expect only qualitative agreement with the data, since our prediction has not been corrected for fragmentation effects. These fragmentation effects are particularly important for small η , so that the nice agreement, in particular for small η 's might be fortuitous.

Acknowledgement. We thank A. Ali for discussions and helpful remarks.

Appendix A

In this appendix we state the analytical result for $D^{3\text{-jet}}(\cos \chi)$ from $d\sigma^{3\text{-jet}}(y)$ of [7]. For convenience, we introduce the abbreviations

$$p_1 = \ln \frac{\zeta}{\eta} \text{atn} \sqrt{\frac{\zeta}{\eta}} - 2 \text{Im Li}_2 \left(i \sqrt{\frac{\zeta}{\eta}} \right) \quad (\text{A.1})$$

$$p_2 = -\ln \frac{\zeta}{\eta} \text{Re Li}_2 \left(i \sqrt{\frac{\zeta}{\eta}} \right) + \text{atn} \sqrt{\frac{\zeta}{\eta}} \text{Im Li}_2 \left(i \sqrt{\frac{\zeta}{\eta}} \right) \\ - 2 \text{Re Li}_3 \left(i \sqrt{\frac{\zeta}{\eta}} \right) + \text{Re S}_{12} \left(i \sqrt{\frac{\zeta}{\eta}} \right) \quad (\text{A.2})$$

where $\zeta = 1 - \eta = \frac{1}{2}(1 - \cos \chi)$. The definitions of the polylogarithms may e.g. be found in [14]. The imaginary and real parts of the polylogarithms can be evaluated to any desired accuracy using the appropriate power expansions. We split $D(\cos \chi)$ into the particular contributions associated to the different colour factors:

$$D^{3\text{-jet}}(\cos \chi) = \frac{C_F}{8\zeta^5 \eta} (C_F D_{C_F} + N_c D_{N_c} + N_f D_{N_f}) \quad (\text{A.3})$$

with

$$D_{C_F} = \ln^2 y [(8\zeta^3 - 36\zeta^2 + 48\zeta - 18) \ln \eta \\ - 18\zeta^3 + 39\zeta^2 - 18\zeta] \\ + \ln y [(34\zeta^3 - 42\zeta^2 + 54\zeta - \frac{61}{3}) \ln \eta \\ + (\frac{2}{3}\zeta^2 + 4\zeta - 16)\zeta \ln \zeta \\ + (-16\zeta^3 + 72\zeta^2 - 84\zeta + 20) \text{Li}_2(\zeta) \\ + (-8\zeta^3 + 36\zeta^2 - 54\zeta + 26) \ln^2 \eta \\ + (12\zeta - 16) \ln \eta \ln \zeta - 47\zeta^3 + \frac{581}{6}\zeta^2 - \frac{121}{3}\zeta] \\ + \pi^2 [(-\frac{4}{3}\zeta^3 + 6\zeta^2 - 6\zeta + \frac{1}{3}) \ln \eta \\ + \frac{28}{9}\zeta^3 - \frac{35}{6}\zeta^2 + \frac{1}{3}\zeta] \\ + (-\frac{55}{9}\zeta^3 + 50\zeta^2 - \frac{361}{6}\zeta + \frac{133}{9}) \ln \eta \\ + (\frac{65}{18}\zeta^2 - \frac{41}{3}\zeta + \frac{31}{3})\zeta \ln \zeta \\ + (\frac{23}{4}\zeta^3 - \frac{111}{4}\zeta^2 + 48\zeta - \frac{10}{3}) \text{Li}_2(\zeta) \\ + (\frac{107}{8}\zeta^3 - \frac{315}{8}\zeta^2 + 44\zeta - 18) \ln^2 \eta \\ + (-\frac{1}{3}\zeta^2 - 2\zeta + 8) \ln^2 \zeta \\ + (-\frac{61}{6}\zeta^3 + \frac{55}{2}\zeta^2 - 28\zeta + \frac{49}{3}) \ln \eta \ln \zeta \\ + (-8\zeta^3 + 54\zeta^2 - 72\zeta + 14) \text{Li}_3(\zeta) \\ + (28\zeta^3 - 102\zeta^2 + 96\zeta - 10) \text{S}_{12}(\zeta) \\ + (-10\zeta^2 + 50\zeta - 70) \ln \eta \text{Li}_2(\zeta) \\ + (8\zeta^3 - 18\zeta^2 - 36\zeta + 58) \ln \zeta \text{Li}_2(\zeta) \\ + (-3\zeta^3 + \frac{1}{2}\zeta^2 + 29\zeta - \frac{59}{2}) \ln^3 \eta \\ + (6\zeta^3 - \frac{27}{2}\zeta^2 - 9\zeta + \frac{39}{2}) \ln^2 \eta \ln \zeta \\ + (-6\zeta + 8) \ln \eta \ln^2 \zeta \\ + (8\zeta^3 - 18\zeta^2 - 12\zeta + 26) \ln \frac{\zeta}{\eta} \text{atn}^2 \sqrt{\frac{\zeta}{\eta}} \\ + (\frac{127}{6}\zeta^2 - \frac{32}{3}\zeta - 52) \sqrt{\zeta \eta} p_1 \\ + (-79\zeta^2 + 212\zeta - 160) \eta \text{Re Li}_2 \left(i \sqrt{\frac{\zeta}{\eta}} \right) \\ + (-32\zeta^3 + 72\zeta^2 + 48\zeta - 104) p_2 \\ - \frac{32}{3}\zeta^3 + \frac{1601}{36}\zeta^2 - \frac{323}{9}\zeta \quad (\text{A.4})$$

$$D_{N_c} = \ln^2 y [(4\zeta^3 - 18\zeta^2 + 24\zeta - 9) \ln \eta \\ - 9\zeta^3 + \frac{39}{2}\zeta^2 - 9\zeta] \\ + \ln y [(-10\zeta^3 + 42\zeta^2 - 52\zeta + \frac{113}{6}) \ln \eta \\ + (\frac{52}{3}\zeta^2 - 43\zeta + 34)\zeta \ln \zeta \\ + (-16\zeta^3 + 72\zeta^2 - 108\zeta + 52) \text{Li}_2(\zeta) \\ + (6\zeta - 8) \ln^2 \eta \\ + (-8\zeta^3 + 36\zeta^2 - 60\zeta + 34) \ln \eta \ln \zeta \\ - \frac{53}{2}\zeta^3 + \frac{725}{12}\zeta^2 - \frac{199}{6}\zeta] \\ + \pi^2 [(-2\zeta^3 + 9\zeta^2 - 14\zeta + \frac{43}{6}) \ln \eta \\ + \frac{79}{18}\zeta^3 - \frac{125}{12}\zeta^2 + \frac{43}{6}\zeta] \\ + (-\frac{883}{36}\zeta^3 + 100\zeta^2 - \frac{1559}{12}\zeta + \frac{479}{9}) \ln \eta \\ + (\frac{329}{36}\zeta^2 - \frac{61}{3}\zeta + \frac{41}{3})\zeta \ln \zeta \\ + (-\frac{25}{2}\zeta^3 - \frac{25}{4}\zeta^2 + \frac{71}{2}\zeta - \frac{365}{12}) \text{Li}_2(\zeta) \\ + (-\frac{53}{4}\zeta^3 + \frac{263}{8}\zeta^2 - \frac{125}{4}\zeta + \frac{105}{8}) \ln^2 \eta$$

* Similar data from the PLUTO collaboration for $E = 34.6 \text{ GeV}$ are published in [13].

$$\begin{aligned}
& + (-\frac{26}{3}\zeta^3 + \frac{43}{2}\zeta - 17)\zeta \ln^2 \zeta \\
& + (\frac{47}{3}\zeta^3 - \frac{115}{2}\zeta^2 + 66\zeta - \frac{85}{3}) \ln \eta \ln \zeta \\
& + (-32\zeta^3 + 135\zeta^2 - 195\zeta + 94) \text{Li}_3(\zeta) \\
& + (-14\zeta^2 + 61\zeta - 62)\eta \mathcal{S}_{12}(\zeta) \\
& + (7\zeta^3 - 24\zeta^2 + 6\zeta + 16) \ln \eta \text{Li}_2(\zeta) \\
& + (16\zeta^3 - 81\zeta^2 + 153\zeta - 94) \ln \zeta \text{Li}_2(\zeta) \\
& + (-\frac{1}{6}\zeta^3 + \frac{29}{4}\zeta^2 - \frac{113}{4}\zeta + \frac{47}{2}) \ln^3 \eta \\
& + (-\frac{27}{4}\zeta^2 + \frac{99}{4}\zeta - \frac{39}{2}) \ln^2 \eta \ln \zeta \\
& + (4\zeta^3 - 18\zeta^2 + 30\zeta - 17) \ln \eta \ln^2 \zeta \\
& + (-9\zeta^2 + 33\zeta - 26) \ln \frac{\zeta}{\eta} \text{atn}^2 \sqrt{\frac{\zeta}{\eta}} \\
& + (\frac{23}{6}\zeta^2 - \frac{94}{3}\zeta + 52) \sqrt{\eta \zeta} p_1 \\
& + (70\zeta^2 - 185\zeta + 133)\eta \text{Re Li}_2\left(i \sqrt{\frac{\zeta}{\eta}}\right) \\
& + (36\zeta^2 - 132\zeta + 104)p_2 \\
& + \frac{221}{12}\zeta^3 - \frac{1613}{36}\zeta^2 + \frac{206}{9}\zeta \tag{A.5}
\end{aligned}$$

$$\begin{aligned}
D_{N_f} = & (\frac{1}{3} \ln y - \frac{5}{9}) [(-4\zeta^3 + 18\zeta^2 - 24\zeta + 9) \ln \eta \\
& + 9\zeta^3 - \frac{39}{2}\zeta^2 + 9\zeta]. \tag{A.6}
\end{aligned}$$

In the back-to-back limiting case ($\eta \rightarrow 0$) this leads to the following asymptotic behaviour:

$$\begin{aligned}
D(\cos \chi \rightarrow -1) & = \frac{C_F}{8\eta} \left\{ \ln^3 \frac{1}{\eta} \left[-\frac{5}{6} N_c \right] + \ln^2 \frac{1}{\eta} \left[-2N_c \ln y + \frac{3}{2} N_c \right] \right. \\
& + \ln \frac{1}{\eta} \left[(-2C_F - N_c) \ln^2 y \right. \\
& + (-3C_F + \frac{7}{6} N_c + \frac{1}{3} N_f) \ln y \\
& + \left. \left. \left(-\frac{\pi^2}{3} + \frac{3}{2} \right) C_F + \left(-\frac{\pi^2}{3} + \frac{11}{9} \right) N_c - \frac{5}{9} N_f \right] \right. \\
& + 3(C_F + \frac{1}{2} N_c) \ln^2 y \\
& + \left. \left[\left(\frac{19}{2} - \frac{4\pi^2}{3} \right) C_F + \frac{3}{4} N_c - \frac{1}{2} N_f \right] \ln y \right. \\
& + \left. \left(\frac{25}{18} \pi^2 - \frac{25}{12} - 16\zeta_3 \right) C_F \right\} \\
& + \left. \left(-\frac{41}{36} \pi^2 - \frac{7}{2} + 10\zeta_3 \right) N_c + \frac{5}{6} N_f \right\} \tag{A.7}
\end{aligned}$$

where only those terms have been kept which diverge at least as fast as η^{-1} . It is interesting to note that the leading y -cut dependence $\sim \ln^2 y$ is only in subleading terms $\sim \ln(1/\eta)/\eta$ and $\sim 1/\eta$. The most singular term $\sim \ln^3(1/\eta)/\eta$ is independent of y . Because of the cut to separate 3- and 4-jet (A.7) shows little similarity to the expansion of the LA in (3.5) and (3.6). In order to obtain all singular terms one must add the genuine 4-jet contributions calculated with the same y cut.

Appendix B

Here we present the contribution to the EEC coming from $d\sigma^3$ plus the singular part of $d\sigma^4$ [9]. Again, we use the notation introduced in (A.1)–(A.3), then the

particular contributions to $D^{3+4s}(\cos \chi)$ read

$$\begin{aligned}
D_{C_F} = & \pi^2 \left[\left(-\frac{4}{3}\zeta^3 + 6\zeta^2 - 9\zeta + \frac{13}{3} \right) \ln \eta \right. \\
& + \frac{53}{18}\zeta^3 - \frac{41}{6}\zeta^2 + \frac{13}{3}\zeta \\
& + \left(\frac{127}{36}\zeta^3 - \frac{85}{12}\zeta^2 + \frac{121}{12}\zeta - \frac{25}{9} \right) \ln \eta \\
& + \left(-\frac{217}{36}\zeta^2 + \frac{39}{4}\zeta + \frac{27}{2} \right) \zeta \ln \zeta \\
& + \left(-\frac{7}{12}\zeta^3 - \frac{213}{4}\zeta^2 + \frac{255}{2}\zeta - 53 \right) \text{Li}_2(\zeta) \\
& + \left(\frac{67}{8}\zeta^3 - \frac{269}{8}\zeta^2 + \frac{169}{4}\zeta - 14 \right) \ln^2 \eta \\
& + \left(\frac{1}{6}\zeta^3 - \frac{27}{2}\zeta^2 + \frac{69}{2}\zeta - \frac{25}{2} \right) \ln \eta \ln \zeta \\
& + \left(-\frac{53}{6}\zeta^2 + \frac{41}{2}\zeta - 13 \right) \zeta \ln^2 \zeta \\
& + (8\zeta^3 - 18\zeta^2 - 12\zeta + 26) \text{Li}_3(\zeta) \\
& + (28\zeta^3 - 102\zeta^2 + 96\zeta - 10) \mathcal{S}_{12}(\zeta) \\
& + (-14\zeta^3 + 48\zeta^2 - 42\zeta + 8) \ln \eta \text{Li}_2(\zeta) \\
& + (24\zeta^3 - 90\zeta^2 + 96\zeta - 26) \ln \zeta \text{Li}_2(\zeta) \\
& + \left(-\frac{31}{3}\zeta^3 + \frac{67}{2}\zeta^2 - \frac{45}{2}\zeta - 3 \right) \ln^3 \eta \\
& + (8\zeta^3 - \frac{45}{2}\zeta^2 + \frac{9}{2}\zeta + 13) \ln^2 \eta \ln \zeta \\
& + (4\zeta^3 - 18\zeta^2 + 27\zeta - 13) \ln \eta \ln^2 \zeta \\
& + (-15\zeta^2 + 54\zeta - 54)\eta \text{Re Li}_2\left(i \sqrt{\frac{\zeta}{\eta}}\right) \\
& + \left(\frac{93}{2}\zeta - 84 \right) \zeta \sqrt{\eta \zeta} p_1 \\
& + (-32\zeta^2 + 108\zeta - 84)\zeta p_2 \\
& + 35\zeta^3 - \frac{3991}{72}\zeta^2 + \frac{193}{18}\zeta \tag{B.1}
\end{aligned}$$

$$\begin{aligned}
D_{N_c} = & \pi^2 \left[\left(\zeta - \frac{4}{3} \right) \ln \eta + \frac{1}{18}\zeta^3 + \frac{1}{3}\zeta^2 - \frac{4}{3}\zeta \right] \\
& + \left(\frac{43}{9}\zeta^3 - \frac{257}{12}\zeta^2 + \frac{82}{3}\zeta - \frac{73}{6} \right) \ln \eta \\
& + \left(-\frac{121}{6}\zeta^2 + \frac{601}{12}\zeta - \frac{215}{6} \right) \zeta \ln \zeta \\
& + \left(-\frac{41}{3}\zeta^3 + \frac{41}{4}\zeta^2 + 17\zeta - \frac{151}{12} \right) \text{Li}_2(\zeta) \\
& + \left(-\frac{40}{3}\zeta^3 + \frac{229}{8}\zeta^2 - 17\zeta + \frac{85}{24} \right) \ln^2 \eta \\
& + \left(\frac{20}{3}\zeta^3 - \frac{45}{2}\zeta^2 + \frac{43}{2}\zeta - \frac{59}{6} \right) \ln \eta \ln \zeta \\
& + \left(-\frac{1}{6}\zeta^2 - \zeta + 4 \right) \zeta \ln^2 \zeta \\
& + (-9\zeta^2 + 33\zeta - 26) \text{Li}_3(\zeta) \\
& + (14\zeta^3 - 75\zeta^2 + 123\zeta - 62) \mathcal{S}_{12}(\zeta) \\
& + (7\zeta^3 - 24\zeta^2 + 24\zeta - 8) \ln \eta \text{Li}_2(\zeta) \\
& + (-9\zeta^2 + 21\zeta - 10) \ln \zeta \text{Li}_2(\zeta) \\
& + \left(\frac{7}{6}\zeta^3 + \frac{5}{4}\zeta^2 - \frac{51}{4}\zeta + \frac{21}{2} \right) \ln^3 \eta \\
& + \left(-\frac{27}{4}\zeta^2 + \frac{93}{4}\zeta - \frac{35}{2} \right) \ln^2 \eta \ln \zeta \\
& + (-3\zeta + 4) \ln \eta \ln^2 \zeta \\
& + (76\zeta^2 - 173\zeta + 121)\eta \text{Re Li}_2\left(i \sqrt{\frac{\zeta}{\eta}}\right) \\
& + \left(\frac{5}{2}\zeta^2 - 30\zeta + 36 \right) \sqrt{\eta \zeta} p_1 \\
& + (18\zeta^2 - 54\zeta + 36)p_2 \\
& + \frac{577}{12}\zeta^3 - \frac{2669}{24}\zeta^2 + \frac{170}{3}\zeta \tag{B.2}
\end{aligned}$$

$$\begin{aligned}
D_{N_f} = & \left(-\frac{13}{18}\zeta^3 + \frac{7}{2}\zeta^2 - \frac{25}{6}\zeta + \frac{13}{9} \right) \ln \eta \\
& + \left(\frac{53}{18}\zeta^2 - \frac{41}{6}\zeta + \frac{13}{3} \right) \zeta \ln \zeta \\
& + (-4\zeta^3 + 18\zeta^2 - 25\zeta + \frac{31}{3}) \text{Li}_2(\zeta) \\
& + \left(-\frac{2}{3}\zeta^3 + 3\zeta^2 - \frac{7}{2}\zeta + \frac{5}{6} \right) \ln^2 \eta \\
& + \left(-\frac{4}{3}\zeta^3 + 6\zeta^2 - 9\zeta + \frac{13}{3} \right) \ln \eta \ln \zeta \\
& - \frac{25}{3}\zeta^3 + \frac{653}{36}\zeta^2 - \frac{80}{9}\zeta. \tag{B.3}
\end{aligned}$$

The asymptotic behaviour for large angles can be extracted to be:

$$\begin{aligned}
D^{3+4s}(\cos \chi \rightarrow -1) &= \frac{C_F}{8\eta} \left\{ \ln^3 \frac{1}{\eta} \left(-\frac{2}{3} C_F - \frac{1}{6} N_c \right) \right. \\
&\quad + \ln^2 \frac{1}{\eta} \left(3C_F + \frac{11}{6} N_c - \frac{1}{3} N_f \right) \\
&\quad + \ln \frac{1}{\eta} \left[-\left(\frac{15}{4} + \frac{4}{3} \pi^2 \right) C_F + \left(\frac{53}{36} + \frac{1}{2} \pi^2 \right) N_c - \frac{1}{18} N_f \right] \\
&\quad + \left(-\frac{233}{24} + \frac{35}{9} \pi^2 \right) C_F + \left(-\frac{155}{24} - \frac{7}{9} \pi^2 - 2\zeta_3 \right) N_c \\
&\quad \left. + \left(\frac{11}{12} - \frac{1}{9} \pi^2 \right) N_f \right\} \quad (\text{B.4})
\end{aligned}$$

where, again, all terms which diverge less than η^{-1} have been neglected. This result shows much more similarity to the $O(\alpha_s^2)$ LA-term in (3.5) (with (3.6)) than the result in Appendix A. This is obvious since (B.4) includes the 4-parton part, although only in the singular approximation, in the whole 4-parton phase space and not only up to the cut y as in (A.7). To obtain the complete large angle behaviour the non-singular 4-parton contribution and a correction, which treats the 4-parton singular part as an EEC correlation involving 4 partons instead of 3 jets, must be added.

$d\sigma^3$ contains an infrared finite contribution coming from loop corrections [6, 9]. This, denoted by $f(x_1, x_2)$, is not accessible for the leading log approximation. For comparison with the LA ($O(\alpha_s) + O(\alpha_s^2)$), this should be subtracted. For this purpose we also give the analytical result for the contribution of f to the EEC:

$$\begin{aligned}
D_{C_F}^f &= \left(-\frac{86}{9} \zeta^3 + 68\zeta^2 - \frac{607}{6} \zeta + \frac{362}{9} \right) \ln \eta \\
&\quad + \left(\frac{55}{18} \zeta^2 - \frac{43}{3} \zeta + 21 \right) \zeta \ln \zeta \\
&\quad + \left(\frac{61}{12} \zeta^3 - \frac{63}{4} \zeta^2 + 40\zeta - 18 \right) \text{Li}_2(\zeta) \\
&\quad + \left(\frac{107}{8} \zeta^3 - \frac{251}{8} \zeta^2 + 22\zeta - 4 \right) \ln^2 \eta \\
&\quad + \left(-\frac{65}{6} \zeta^3 + \frac{47}{2} \zeta^2 - 2\zeta - 5 \right) \ln \eta \ln \zeta \\
&\quad + \left(8\zeta^3 - 18\zeta^2 - 12\zeta + 26 \right) \text{Li}_3(\zeta) \\
&\quad + \left(12\zeta^3 - 30\zeta^2 + 12\zeta + 10 \right) S_{12}(\zeta) \\
&\quad + \left(-6\zeta^3 + 12\zeta^2 + 24\zeta - 34 \right) \ln \eta \text{Li}_2(\zeta) \\
&\quad + \left(8\zeta^3 - 18\zeta^2 - 12\zeta + 26 \right) \ln \zeta \text{Li}_2(\zeta) \\
&\quad + \left(-\frac{17}{3} \zeta^3 + \frac{25}{2} \zeta^2 + 11\zeta - \frac{125}{6} \right) \ln^3 \eta \\
&\quad + \left(6\zeta^3 - \frac{27}{2} \zeta^2 - 9\zeta + \frac{39}{2} \right) \ln^2 \eta \ln \zeta \\
&\quad + \left(-79\zeta^2 + 212\zeta - 160 \right) \eta \text{Re Li}_2 \left(i \sqrt{\frac{\zeta}{\eta}} \right) \\
&\quad + \left(\frac{127}{8} \zeta^2 - \frac{32}{3} \zeta - 52 \right) \sqrt{\zeta} \eta p_1 \\
&\quad + \left(-16\zeta^3 + 36\zeta^2 + 24\zeta - 52 \right) p_2 \\
&\quad + \frac{49}{3} \zeta^3 - \frac{599}{36} \zeta^2 - \frac{70}{9} \zeta \quad (\text{B.5}) \\
D_{N_c}^f &= \left(\frac{173}{36} \zeta^3 - \frac{33}{2} \zeta^2 + \frac{257}{12} \zeta - \frac{92}{9} \right) \ln \eta \\
&\quad + \left(-\frac{191}{36} \zeta^2 + \frac{71}{6} \zeta - 12 \right) \zeta \ln \zeta \\
&\quad + \left(-\frac{179}{6} \zeta^3 + \frac{371}{4} \zeta^2 - \frac{237}{2} \zeta - \frac{189}{4} \right) \text{Li}_2(\zeta) \\
&\quad + \left(-\frac{53}{4} \zeta^3 + \frac{295}{8} \zeta^2 + \frac{133}{4} \zeta + \frac{77}{8} \right) \ln^2 \eta \\
&\quad + \left(-\frac{5}{3} \zeta^3 + \frac{19}{2} \zeta^2 - 26\zeta + 14 \right) \ln \eta \ln \zeta
\end{aligned}$$

$$\begin{aligned}
&+ \left(-9\zeta^2 + 33\zeta - 26 \right) \text{Li}_3(\zeta) \\
&+ \left(-2\zeta^3 - 3\zeta^2 + 15\zeta - 10 \right) S_{12}(\zeta) \\
&+ \left(-\zeta^3 + 12\zeta^2 - 42\zeta + 34 \right) \ln \eta \text{Li}_2(\zeta) \\
&+ \left(-9\zeta^2 + 33\zeta - 26 \right) \ln \zeta \text{Li}_2(\zeta) \\
&+ \left(-\frac{1}{6} \zeta^3 + \frac{29}{4} \zeta^2 - \frac{105}{4} \zeta - \frac{125}{6} \right) \ln^3 \eta \\
&+ \left(-\frac{27}{4} \zeta^2 - \frac{99}{4} \zeta - \frac{39}{2} \right) \ln^2 \eta \ln \zeta \\
&+ \left(70\zeta^2 - 185\zeta + 133 \right) \eta \text{Re Li}_2 \left(i \sqrt{\frac{\zeta}{\eta}} \right) \\
&+ \left(\frac{23}{6} \zeta^2 - \frac{94}{3} \zeta + 52 \right) \sqrt{\eta} \zeta p_1 \\
&+ \left(18\zeta^2 - 66\zeta + 52 \right) p_2 \\
&- \frac{73}{12} \zeta^3 + \frac{44}{9} \zeta^2 + \frac{16}{9} \zeta. \quad (\text{B.6})
\end{aligned}$$

For $\eta \rightarrow 0$, the $O(\alpha_s^2)$ loop contribution to the EEC has the asymptotic behaviour:

$$\begin{aligned}
D^f(\cos \chi \rightarrow -1) &= \frac{C_F}{8\eta} \left\{ \ln^3 \frac{1}{\eta} \left(-\frac{1}{6} N_c \right) \right. \\
&\quad + \ln \frac{1}{\eta} \left[\left(\frac{5}{2} - \frac{2}{3} \pi^2 \right) C_F + \left(\frac{1}{2} + \frac{1}{6} \pi^2 \right) N_c \right] \\
&\quad + \left(-\frac{97}{12} + \frac{17}{9} \pi^2 - 8\zeta_3 \right) C_F \\
&\quad \left. + \left(\frac{7}{12} - \frac{25}{8} \pi^2 + 6\zeta_3 \right) N_c \right\}. \quad (\text{B.7})
\end{aligned}$$

The result (B.7) shows that the N_c -term proportional to $\ln^3(1/\eta)$ in (B.4) originates from the contribution (B.6), i.e. non-infrared virtual corrections. It is difficult to believe that such a term is contained in the usual logarithmic approximation. If also the $C_F N_c \ln(1/\eta)/16\eta$ is subtracted in (B.4) another term agrees with the logarithmic approximation (3.5).

References

1. C.L. Basham, L.S. Brown, S.D. Ellis, S.T. Love: Phys. Rev. D17 (1978) 2298; Phys. Rev. Lett. 41 (1978) 1585; Phys. Rev. D19 (1979) 2018
2. A. Ali, F. Barreiro: Phys. Lett. B118 (1982) 155; Nucl. Phys. B236 (1984) 269
3. S.D. Ellis, D.G. Richards, W.J. Stirling: Phys. Lett. B136 (1984) 99; D.G. Richards, W.J. Stirling, S.D. Ellis: Nucl. Phys. B229 (1983) 317
4. H.N. Schneider, G. Kramer, G. Schierholz: Z. Phys. C—Particles and Fields 22 (1984) 201
5. S.D. Ellis, W.J. Stirling: Phys. Rev. D23 (1981) 214; S.D. Ellis, N. Fleishon, W.J. Stirling: Phys. Rev. D24 (1981) 1386; J.C. Collins, D.E. Soper: Nucl. Phys. B193 (1981) 381; B197 (1982) 446; B213 (1983) 545
6. K. Fabricius, G. Kramer, G. Schierholz, I. Schmitt: Z. Phys. C—Particles and Fields 11 (1982) 315
7. F. Gutbrod, G. Kramer, G. Schierholz: Z. Phys. C—Particles and Fields 21 (1984) 235
8. G. Kramer, B. Lampe: DESY-Report 86-119, 1986 and Fortschr. Phys. (to be published)
9. R.K. Ellis, D.A. Ross, A.E. Terrano: Nucl. Phys. B178 (1981) 421
10. S.D. Ellis, W.J. Stirling: [5]; S.D. Ellis, N. Fleishon, W.J. Stirling: [5]
11. J.C. Collins, D.E. Soper: Nucl. Phys. B284 (1987) 253 and earlier papers cited there
12. W. Braunschweig et al.: Z. Phys. C—Particles and Fields 36 (1987) 349
13. Ch. Berger et al.: Z. Phys. C—Particles and Fields 28 (1985) 365
14. A. Devoto, D.W. Duke: Riv. Nuovo Cimento 7 (1984) 1